

Optics Letters

Quasi-phase-matched multispectral Kerr frequency comb

SHU-WEI HUANG,^{1,*} ABHINAV KUMAR VINOD,¹ JINGHUI YANG,¹ MINGBIN YU,²
DIM-LEE KWONG,² AND CHEE WEI WONG¹

¹Fang Lu Mesoscopic Optics and Quantum Electronics Laboratory, University of California Los Angeles, Los Angeles, California 90095, USA

²Institute of Microelectronics, Singapore, Singapore

*Corresponding author: swhuang@seas.ucla.edu

Received 15 March 2017; revised 25 April 2017; accepted 25 April 2017; posted 1 May 2017 (Doc. ID 290523); published 24 May 2017

We study a new type of Kerr frequency comb where the momentum conservation law is fulfilled by azimuthal modulation of the waveguide dispersion. The concept can expand the parametric range in which a Kerr frequency comb is obtained. In a good agreement with the theoretical analysis, we demonstrate a multispectral Kerr frequency comb covering important fiber-optic communication bands. Comb coherence and absence of a sub-comb offset are confirmed by continuous-wave heterodyne beat note and amplitude noise spectra measurements. The device can be used for achieving broadband optical frequency synthesizers and high-capacity coherent communication. © 2017 Optical Society of America

OCIS codes: (130.0130) Integrated optics; (140.3948) Microcavity devices; (190.0190) Nonlinear optics.

<https://doi.org/10.1364/OL.42.002110>

Optical frequency combs, with precisely controlled spectral lines spanning a broad range, have made great impacts on frequency metrology, optical clockwork, precision navigation, and molecular fingerprinting. In addition to the standard implementation based on mode-locked lasers, optical frequency combs based on parametric oscillations in ultrahigh- Q microresonators have become invaluable in applications requiring a compact footprint, low power consumption, large comb spacing, and access to nonconventional spectral regions. Recent demonstrations of low-phase-noise photonic oscillators [1,2], high-repetition-rate femtosecond pulse trains [3–6], phase stabilized microcombs [7,8], and coherent optical communication [9] have revealed the outstanding performance of these so-called Kerr frequency combs, and reassured further expansion of already remarkable applications.

For efficient Kerr frequency comb generation, both the energy and the momentum conservation laws must be satisfied. In general, the azimuthal mode numbers (N) of the signal and idler are symmetrically located with respect to the pump mode (ω_0), and thus it requires either an intricate balance between the anomalous group velocity dispersion (GVD, β_2) and the nonlinear mode pulling effect, or a careful design of the GVD spectral profile, considering higher-order dispersions,

to satisfy both conservation laws [10,11]. In this Letter, we examine a distinctly different method to fulfill the momentum conservation law, or the phase-matching condition, and demonstrate a new type of multispectral Kerr frequency comb.

Here, we consider the case in which the azimuthal mode numbers of the signal and idler are not symmetrically located with respect to the pump mode. Figure 1(a) illustrates an example in which the resonator exhibits only a normal GVD and no higher-order dispersions. Away from the pump mode, the free spectral ranges (FSRs) on the signal and idler sides monotonically decrease and increase by $D_2 = -\frac{\beta_2 c FSR_0^2}{n}$ per mode, where c is the speed of light and n is the refractive index, respectively. The mismatch between the signal-pump and pump-idler detuning increases as a quadratic function of the azimuthal mode number, eventually approaching the FSR of the $(N + 1)$ th signal mode at $N = \left\lceil \sqrt{\frac{FSR_0}{-D_2}} - 1 \right\rceil$, i.e., $(\omega_N - \omega_0) - (\omega_0 - \omega_{-N}) = -FSR_{N+1}$. Consequently, the energy conservation law of $\omega_{N+1} + \omega_{-N} - 2 \cdot \omega_0 = 0$ is satisfied. Here ω_N represents the resonance frequency of the N th azimuthal cavity mode. On the other hand, the asymmetry in the signal and idler mode numbers renders the momentum conservation law violated unless an azimuthal modulation of the cavity parameters is introduced to provide an additional wavevector for quasi-phase matching (QPM). The spontaneous pattern formation mediated by a periodic modulation of system parameters is mathematically equivalent to the formation of Faraday ripples, first observed in hydrodynamics and recently expanded to fiber nonlinear optics [12–16]. Our use of a Si_3N_4 planar microresonator has the advantage of straightforward dispersion management by the design of waveguide geometry [Fig. 1(b)], opening up the possibility of implementing the QPM concept via azimuthal GVD modulation. The inset of Fig. 1(b) schematically shows a dispersion-modulated single-mode Si_3N_4 microresonator, which consists of adiabatically tapered waveguides in the straight region that yield GVD oscillations in the -40 to 140 fs^2/mm range, and uniform single-mode waveguides in the semi-circular region that ensure no excitation of higher-order transverse modes. The resonator geometry and fabrication is identical to the one shown in Ref. [17], but the pump now is TM polarized.

Kerr frequency comb generation in these continuous-wave (cw)-laser-pumped nonlinear microresonators is described by the Lugiato–Lefever equation [16,18–20]

$$\frac{\partial}{\partial Z} A = \sqrt{T_c} A_p - \left(\alpha + \frac{T_c}{2} + i\delta + i\gamma L |A|^2 \right) A + \frac{i\beta_2(Z)L}{2} \frac{\partial^2 A}{\partial t^2}, \quad (1)$$

where $A(Z, t)$ is the envelope function of the intra-cavity electric field, T_c is the power coupling loss, α is the amplitude attenuation per roundtrip, δ is the pump-resonance detuning, γ is the nonlinear coefficient, L is the cavity length, and $\beta_2(Z)$ is the GVD profile within the cavity. Of note, the GVD periodicity is guaranteed by the cavity to be L . Assuming a piecewise constant GVD profile with a duty cycle of 50%, for simplicity, and following the procedures outlined in Ref. [16], we can analytically evaluate the gain of Faraday ripples as a function of the sideband frequency and intra-cavity pump power [Fig. 1(c)]. Furthermore, the gain peak sideband frequency can be expressed analytically as

$$\omega_F = \sqrt{\frac{2 \left[\left(\frac{\delta}{L} - 2\gamma P_{\text{in}} \right) \pm \sqrt{(\gamma P_{\text{in}})^2 + \left(\frac{\delta}{L} \right)^2} \right]}{\beta_2}}, \quad (2)$$

where $P_{\text{in}} = |A_{\text{in}}|^2$ is the intra-cavity pump power and $\overline{\beta_2}$ is the path-averaged GVD. Under the mean field and good cavity approximations [21], i.e., assuming γP_{in} , $\delta \sim O(\epsilon)$, Eq. (2) reduces to

$$\overline{\beta_2} \omega_F^2 = \eta \cdot 2 \frac{\pi}{L}, \quad (3)$$

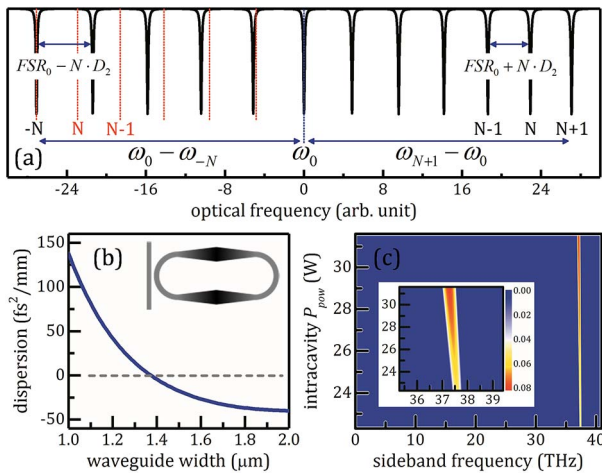


Fig. 1. (a) Principle of the QPM Kerr frequency comb generation, assuming that the azimuthal mode numbers of the signal and idler are not symmetrically located with respect to the pump mode. The momentum conservation law is always violated unless an azimuthal modulation of the cavity parameters is introduced to provide an additional wavevector for the QPM condition. The red dashed lines show the resonance frequencies that are mirrors of the signal modes with respect to the pump mode. (b) COMSOL-modeled GVD of the Si₃N₄ waveguide with respect to the waveguide width. Inset: schematic of our dispersion-modulated single-mode Si₃N₄ microresonator. (c) Analytic gain of Faraday ripples as a function of the sideband frequency and intra-cavity pump power. Inset: zoom-in map of the roundtrip gain coefficient, showing the gain peak at ~37.5 THz.

where $\eta = \pm 1$ depending on the sign of $\overline{\beta_2}$. Equation (3) explicitly shows how the GVD-induced phase mismatch (left-hand side) can be compensated by the additional wavevector provided by the azimuthal GVD modulation (right-hand side). Such an additional wavevector enables efficient sideband generation even in normal GVD microresonators without any higher-order dispersions, thereby expanding the parametric range of the Kerr frequency comb.

Figure 2(a) shows the path-averaged GVD and third-order dispersion (TOD) of our dispersion-modulated single-mode microresonator, simulated using COMSOL Multiphysics [17]. The GVD remains normal while the TOD is anomalous across the entire fiber-optic communication C/L band (1530–1625 nm), with GVD = 50 fs²/mm and TOD = -1160 fs³/mm at

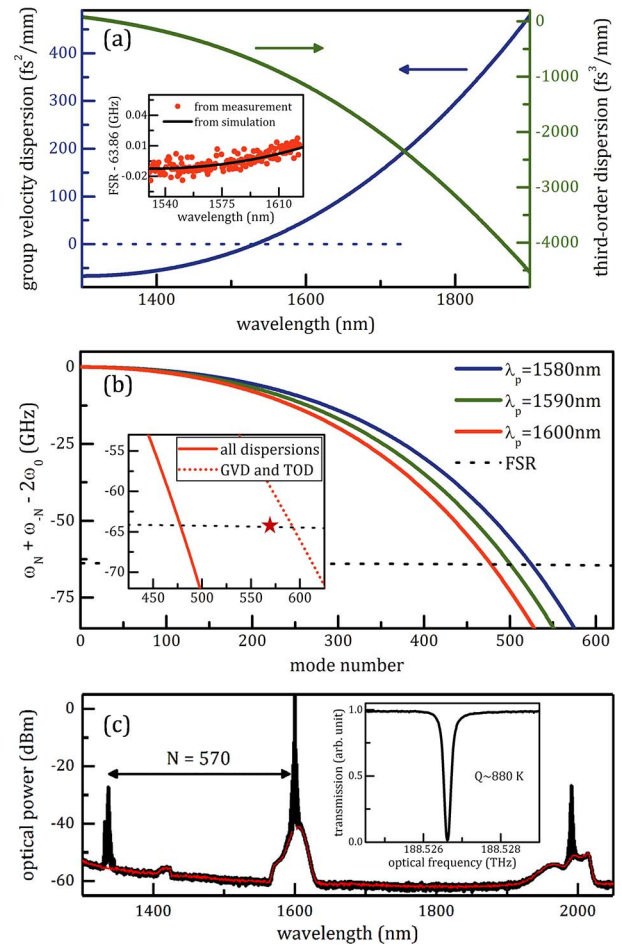


Fig. 2. (a) Path-averaged GVD and TOD of the microresonator, showing a monotonic GVD change from 20 fs²/mm at 1560 nm to 50 fs²/mm at 1600 nm. Inset: measured wavelength-dependent FSRs (red dots), showing a good agreement with the simulation results (black line). (b) Mismatch between the signal-pump and pump-idler detuning and the FSR, as a function of the azimuthal mode number. The crossing between the mismatch and the FSR denotes the region in which the first QPM sideband pairs are expected to emerge. Inset: magnified view, showing the experimentally measured point (star) between the values numerically obtained with (solid line) and without (dashed line) higher-order dispersions. (c) Example optical spectrum of Faraday ripples pumped at 1600 nm, showing the first sideband pair at the azimuthal mode $N = 570$. Red dotted line is the OSA's background noise. Inset: a loaded Q of 880,000 is measured at 1600 nm.

1600 nm. A high-resolution coherent swept wavelength interferometer is used to characterize the cold cavity properties of the designed microresonator [17]. The measured wavelength-dependent FSRs, overlaid with the results of simulations accounting for both the GVD and the TOD, are shown in the inset of Fig. 2(a). A good agreement between the experimental and simulation results is achieved. Figure 2(b) shows the mismatch between the signal-pump and pump-idler detuning, $\omega_N + \omega_{-N} - 2 \cdot \omega_0$, as well as the FSR as a function of the azimuthal mode number. The crossing between the mismatch and the FSR denotes the region in which the first QPM Kerr frequency comb sidebands are expected to emerge. For the pump wavelength of 1600 nm, the numerical calculation predicts the sideband mode number $N = 480$, while the experimentally measured sidebands are clustered around $N = 570$ [Fig. 2(c)]. On the other hand, if dispersion orders higher than TOD are not considered in the numerical calculation, the obtained sideband mode number is $N = 590$ [red dashed line in the inset of Fig. 2(b)] and a better agreement with the experimental sideband mode number is obtained. Thus, we attribute this discrepancy to the uncertainty of dispersion orders higher than TOD in the numerical simulation.

The frequency of the Faraday ripples, or primary comb spacing, can be tuned by changing the pump frequency. As the pump frequency increases, the GVD decreases monotonically,

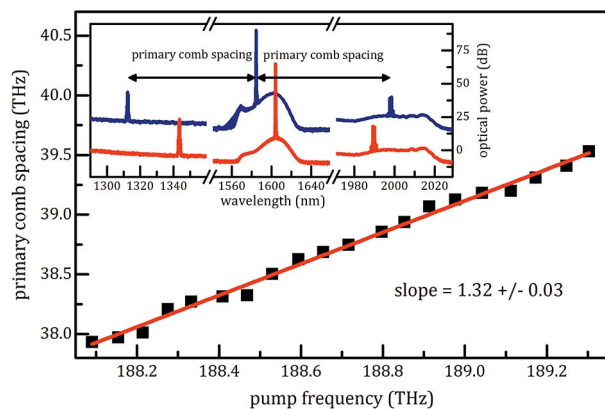


Fig. 3. Frequency of the Faraday ripples is linearly related to the pump frequency with a fitted slope of 1.32 ± 0.3 , well matching the numerically calculated slope of 1.27. Inset: example optical spectra of the Faraday ripples pumped at 1585 nm (blue line) and 1605 nm (red line).

resulting in a positive correlation between the primary comb spacing and the pump frequency, according to Eq. (2). Figure 3 shows this correlation, obtained by pumping the microresonator's 20 different modes around 1590 nm and measuring the primary comb spacing using a high-resolution optical spectrum analyzer (OSA). Linear regression analysis on the measured data yields a good adjusted R-squared value of 99.3%. The fitted slope is 1.32 ± 0.3 , well matching the slope of 1.27 predicted from the numerical calculation [Fig. 2(b)]. Setting the pump frequency to 189.8 THz results in the primary comb spacing of 40.2 THz, with the overall bandwidth spanning 2/3 of an octave. By pumping the microresonator two times harder with an on-chip pump power of 30 dBm, subsequent non-degenerate four-wave mixing occurs, forming secondary comb lines, and three broadband Kerr frequency combs are formed, with center wavelengths of 1304 nm, 1580 nm, and 2002 nm (Fig. 4). With its optical power concentrated on the two spectral edges, the broadband Kerr frequency comb, once merged, is expected to be advantageous for reducing the complexity of the microresonator self-referencing scheme [8]. Importantly, each segment of the multispectral Kerr frequency comb covers an important fiber-optic communication band, including the traditional O (1260–1360 nm) and C/L bands as well as the emerging 2- μ m channel that is compatible with group IV photonics [22]. Both the O band and the C/L band Kerr frequency combs span more than 8 THz, while the 2 μ m Kerr frequency comb spans a narrower 4 THz owing to the aberration in the near infrared (NIR) coupling optics. The comb span is defined as the bandwidth in which the comb power remains higher than the OSA noise level of -60 dBm. Furthermore, characteristics of the O band and the C/L band Kerr frequency combs are individually investigated by performing cw heterodyne beat note measurements and by measuring amplitude noise spectra with a scan range much wider than the cavity linewidth [6,23]. An independent narrow-linewidth tunable laser is used as an optical reference to generate heterodyne beat notes with the pump laser and different comb lines in the C/L band and the O band (Fig. 5). All beat notes exhibit the same linewidth of 350 kHz, limited by the mutual coherence between the reference laser and the pump laser. Neither additional linewidth broadening of the comb lines relative to the pump nor multiple beat notes is observed, confirming that the comb lines exhibit a similar level of phase noise as the pump. Besides good comb line coherence, the absence of comb breathing and a sub-comb

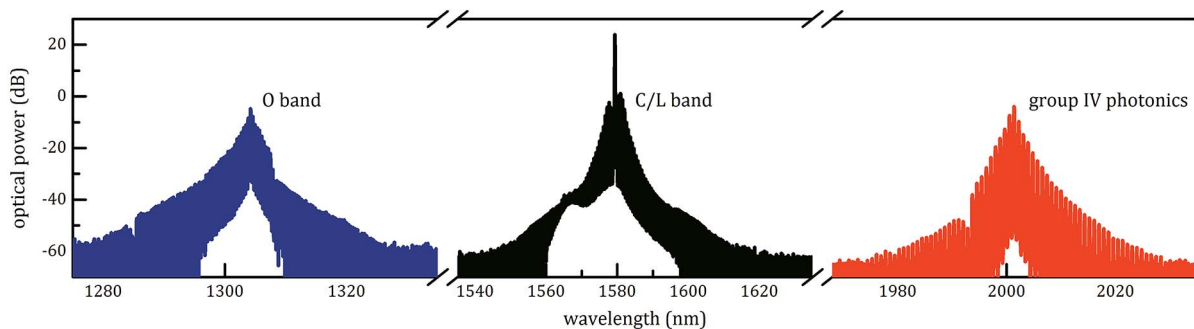


Fig. 4. QPM multispectral Kerr frequency comb covers important fiber-optic communication bands, including the emerging 2- μ m channel that is compatible with group IV photonics. Both the O band and the C/L band combs span more than 8 THz above the OSA noise floor, while the 2- μ m comb spans a narrower 4 THz owing to the aberration in the NIR coupling optics. The overall bandwidth spans more than 2/3 of an octave.

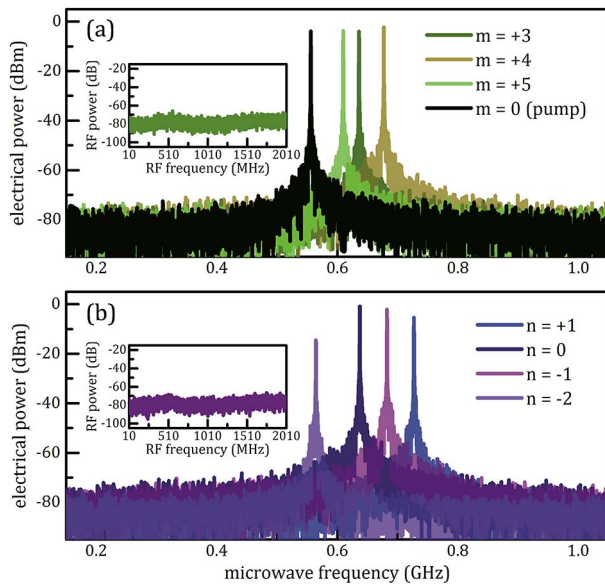


Fig. 5. (a) Heterodyne beat notes and RF amplitude noise spectrum (inset) of the C/L band Kerr frequency comb. $m = 0$ corresponds to the pump mode at 1580 nm. (b) Heterodyne beat notes and RF amplitude noise spectrum (inset) of the O band Kerr frequency comb. $n = 0$ corresponds to the comb line at 1304 nm.

offset is also important, as they degrade the quality of optical communication [24]. It is independently confirmed by performing amplitude noise measurements (insets of Fig. 5), and no peaks or excess noise are observed for frequencies reaching up to 2010 MHz (about ten times the cavity linewidth). Different from the traditional Kerr frequency comb formation dynamics where the growth of secondary comb lines is associated with high-noise incoherent chaos [23], here the coherence of the QPM Kerr frequency comb remains without destabilization into chaos. The rigorous physical understanding of such a phenomenon is still under investigation.

In summary, we examine and demonstrate the first QPM Kerr frequency comb where the momentum conservation law is satisfied by azimuthal modulation of the waveguide dispersion. The concept expands the parametric range in which a Kerr frequency comb is obtained. Our use of a Si_3N_4 planar microresonator has the advantage of straightforward dispersion management by the design of waveguide geometry; the same principle can be applied to other types of microresonators by engineering the cavity structures [25–27]. In addition, it has been shown theoretically that periodic pump injection can also generate Faraday ripples at high powers [28]. Choosing a proper pump frequency, we demonstrate a multispectral Kerr frequency comb with the overall bandwidth spanning $2/3$ of an octave and covering multiple important fiber-optic communication bands. In addition, we confirm the comb coherence as well as the absence of comb breathing and a sub-comb offset, by performing cw heterodyne beat note and amplitude noise spectra measurements. The reported QPM multispectral Kerr frequency comb is a promising platform for broadband optical frequency synthesizers and high-capacity coherent communication.

Funding. Air Force Office of Scientific Research (AFOSR) (FA9550-15-1-0081); Office of Naval Research (ONR) (N00014-14-1-0041).

REFERENCES

- S.-W. Huang, J. Yang, J. Lim, H. Zhou, M. Yu, D.-L. Kwong, and C. W. Wong, *Sci. Rep.* **5**, 13355 (2015).
- W. Liang, D. Eliyahu, V. S. Ilchenko, A. A. Savchenkov, A. B. Matsko, D. Seidel, and L. Maleki, *Nat. Commun.* **6**, 7957 (2015).
- K. Saha, Y. Okawachi, B. Shim, J. S. Levy, R. Salem, A. R. Johnson, M. A. Foster, M. R. E. Lamont, M. Lipson, and A. L. Gaeta, *Opt. Express* **21**, 1335 (2013).
- T. Herr, V. Brasch, J. D. Jost, C. Y. Wang, N. M. Kondratiev, M. L. Gorodetsky, and T. J. Kippenberg, *Nat. Photonics* **8**, 145 (2013).
- X. Xue, Y. Xuan, Y. Liu, P.-H. Wang, S. Chen, J. Wang, D. E. Leaird, M. Qi, and A. M. Weiner, *Nat. Photonics* **9**, 594 (2015).
- S.-W. Huang, H. Zhou, J. Yang, J. F. McMillan, A. Matsko, M. Yu, D.-L. Kwong, L. Maleki, and C. W. Wong, *Phys. Rev. Lett.* **114**, 053901 (2015).
- S.-W. Huang, J. Yang, M. Yu, B. H. McGuyer, D.-L. Kwong, T. Zelevinsky, and C. W. Wong, *Sci. Adv.* **2**, e1501489 (2016).
- P. Del'Haye, A. Coillet, T. Fortier, K. Beha, D. C. Cole, K. Y. Yang, H. Lee, K. J. Vahala, S. B. Papp, and S. A. Diddams, *Nat. Photonics* **10**, 516 (2016).
- J. Pfeifle, V. Brasch, M. Lauerer, Y. Yu, D. Wegner, T. Herr, K. Hartinger, P. Schindler, J. Li, D. Hillerkuss, R. Schmogrow, C. Weimann, R. Holzwarth, W. Freude, J. Leuthold, T. J. Kippenberg, and C. Koos, *Nat. Photonics* **8**, 375 (2014).
- A. B. Matsko, A. A. Savchenkov, S.-W. Huang, and L. Maleki, *Opt. Lett.* **41**, 5102 (2016).
- M. H. P. Pfeiffer, C. Herkommer, J. Liu, H. Guo, M. Karpov, E. Lucas, M. Zervas, and T. J. Kippenberg, "Octave-spanning dissipative Kerr soliton frequency combs in Si_3N_4 microresonators," arXiv:1701.08594 (2017).
- M. Droques, A. Kudlinski, G. Bouwmans, G. Martinelli, and A. Mussot, *Opt. Lett.* **37**, 4832 (2012).
- C. Finot, J. Fatome, A. Sysoliatin, A. Kosolapov, and S. Wabnitz, *Opt. Lett.* **38**, 5361 (2013).
- M. Conforti, A. Mussot, A. Kudlinski, and S. Trillo, *Opt. Lett.* **39**, 4200 (2014).
- N. Tarasov, A. M. Perego, D. V. Churkin, K. Staliunas, and S. K. Turitsyn, *Nat. Commun.* **7**, 12441 (2016).
- F. Copie, M. Conforti, A. Kudlinski, A. Mussot, and S. Trillo, *Phys. Rev. Lett.* **116**, 143901 (2016).
- S.-W. Huang, H. Liu, J. Yang, M. Yu, D.-L. Kwong, and C. W. Wong, *Sci. Rep.* **6**, 26255 (2016).
- M. Haelterman, S. Trillo, and S. Wabnitz, *Opt. Lett.* **17**, 745 (1992).
- Y. K. Chembo and C. R. Menyuk, *Phys. Rev. A* **87**, 053852 (2013).
- S. Coen, H. G. Randle, T. Sylvestre, and M. Erkintalo, *Opt. Lett.* **38**, 37 (2013).
- S. Coen and M. Haelterman, *Phys. Rev. Lett.* **79**, 4139 (1997).
- R. Soref, *Nat. Photonics* **9**, 358 (2015).
- T. Herr, K. Hartinger, J. Riemensberger, C. Y. Wang, E. Gavartin, R. Holzwarth, M. L. Gorodetsky, and T. J. Kippenberg, *Nat. Photonics* **6**, 480 (2012).
- C. Bao, P. Liao, L. Zhang, Y. Yan, Y. Cao, G. Xie, A. Mohajerin-Ariaei, L. Li, M. Ziyadi, A. Almaini, L. C. Kimerling, J. Michel, and A. E. Willner, *Opt. Lett.* **41**, 1764 (2016).
- L. Zhang, A. M. Agarwal, L. C. Kimerling, and J. Michel, *Nanophotonics* **3**, 247 (2014).
- I. S. Grudin and N. Yu, *Optica* **2**, 221 (2015).
- K. Y. Yang, K. Beha, D. C. Cole, X. Yi, P. Del'Haye, H. Lee, J. Li, D. Y. Oh, S. A. Diddams, S. B. Papp, and K. J. Vahala, *Nat. Photonics* **10**, 316 (2016).
- T. Hansson and S. Wabnitz, *J. Opt. Soc. Am. B* **32**, 1259 (2015).